



Fluorinate a Polymer Donor through Trifluoromethyl Group for High-Performance Polymer Solar Cells

Journal:	<i>Journal of Materials Chemistry A</i>
Manuscript ID	TA-ART-01-2020-000098.R1
Article Type:	Paper
Date Submitted by the Author:	20-May-2020
Complete List of Authors:	Meng, Hong; Peking University, Yao, Chao; School of Advanced Materials, Peking University Shenzhen Graduate School, Peking University, Shenzhen Zhu, Yanan; Peking University Shenzhen Graduate School Gu, Kaichen; Princeton University, Chemical and Biological Engineering Zhao, Jia; School of Advanced Materials, Peking University Shenzhen Graduate School, Peking University, Shenzhen Ning, Jiaoyi; School of Advanced Materials, Peking University Shenzhen Graduate School, Peking University Perepichka, Dmitrii; McGill University, Chemistry Loo, Yueh-Lin; Princeton University, Department of Chemical Engineering

Fluorinate a Polymer Donor through Trifluoromethyl Group for High-Performance Polymer Solar Cells

*Chao Yao, Yanan Zhu, Kaichen Gu, Jiajun Zhao, Jiaoyi Ning, Dmitrii F. Perepichka, Yueh-Lin Loo, Hong Meng **

C. Yao, Y. N. Zhu, J. J. Zhao, J. Y. Ning, Prof. H. Meng

School of Advanced Materials
Peking University Shenzhen Graduate School
Shenzhen, 518055, China
E-mail: menghong@pku.edu.cn

K. Gu, Prof. Y.-L. Loo
Department of Chemical and Biological Engineering
Princeton University
Princeton, New Jersey 08544, United States

Prof. Y.-L. Loo
Andlinger Center for Energy and the Environment
Princeton University
Princeton, New Jersey 08544, United States

Prof. D.-F. Perepichka
Department of Chemistry and Centre for Self-Assembled Chemical Structures
McGill University
801 Sherbrooke Street West, Montreal, H3A0B8, QC, Canada.

Abstract

Aromatically fluorinated polymers, which have been widely used in highly efficient polymer solar cells (PSCs), suffer from complicated synthesis and low yields. Herein, through replacing methyl group with trifluoromethyl group, the feasibility of synthetically-simple non-aromatic fluorination towards high-performance polymer donors is demonstrated. Two structurally similar polymer donors, one having a trifluoromethyl (-CF₃) group, and the other a methyl (-CH₃) pendant group for comparison, were designed and synthesized. By comparing these two donors, we found the -CF₃ group addition to lower the HOMO energy level, increase absorption through improved intermolecular interactions. Single-junction solar cells based on the trifluoromethylated donor yield a maximum power conversion efficiency of 13.5%, representing a nearly two-fold increase

compared with that of devices using the methylated counterpart. These findings reveal great potential to improve solar cell performance through fluorinating polymer donors by trifluoromethyl group.

Introduction

Polymer solar cells (PSCs) with a bulk heterojunction (BHJ) architecture have attracted much attention given their promise as components for large-area flexible solar panels that can be fabricated through low-cost solution coating techniques^{1, 2}. Recent developments in polymer donors³ and non-fullerene acceptors⁴⁻¹⁰ have led to dramatic increases in performance with power-conversion efficiencies (PCEs) over 16%^{11, 12}. Ideally, the polymer donor should exhibit complementary absorption profile to that of the acceptor to maximize photo-absorption and current generation. Adding to this selection rule is the need for the energy levels of the polymer donor to be appropriately aligned with those of the electron acceptor to provide a small but sufficient offset to facilitate efficient exciton dissociation while minimizing energy loss during photocurrent generation¹³⁻¹⁹. In addition, favorable mixing behavior of donor and acceptor to form a nanoscale bi-continuous interpenetrating network facilitates charge separation. Finally, balanced electron/hole mobility of donor/acceptor blends is critical for efficient charge transport.

Many design strategies have been developed to alter the optoelectronic properties of the polymer donor so it meets the requirements above. For example, changing the backbone constituent from benzene moieties to thiophene moieties, tuning side groups from alkyl chains to thienyl chains and adjusting energy levels through introducing electron-withdrawing or electron-donating groups, have been reported to impact the macroscopic properties of polymer donors.^{3, 20-22} Particularly, introducing fluorine (F) atoms on the conjugated backbone or on the side chain of conjugated polymers has been shown to improve the efficiencies of PSCs when these polymers, as opposed to their unfluorinated counterparts, are introduced as donors. This strategy is based on a high electronegativity of fluorine (4.0 in Pauling scale) which withdraws the electron density from the polymer backbone through an inductive effect, although this effect is partially compensated by resonance electron-donating effect due to interactions of fluorine's lone electron pairs with the π -conjugated system. The overall effect of introducing F atoms is lowering the highest occupied

molecular orbital (HOMO) and the lowest unoccupied molecular orbital (LUMO). Consequently, this functionalization strategy has often resulted in improving the open circuit voltage (V_{OC}) of the resulting PSCs.¹⁸ Additionally, fluorine can modulate the intermolecular interactions of conjugated polymers by altering their dipole moments, resulting in vastly different aggregation behavior.¹⁷

Generally, fluorine is introduced through aromatic fluorination reactions, which require multiple synthetic steps and tedious purification procedures^{23, 24}. Here, aromatic fluorination happens when an aromatic hydrogen atom is substituted by a fluorine atom. As a result, the synthesis of such fluorinated donor materials is costly and time consuming. In order to simplify synthesis, efforts devoted to replacing -F in polymer donors with other readily-introduced electron-deficient groups, like chlorine, cyano, sulfonyl, and so on, have been reported.^{20, 25, 26} However, the PSCs that incorporate these non-fluorinated polymers as donors do not exhibit PCEs as high as those using fluorinated polymers. Hence, it is critical to find an alternative to fluorine substituents without increasing the synthetic complexity.

Trifluoromethylated compounds have found many industrial applications ranging from dyes to pharmaceuticals and agrochemicals. The trifluoromethyl group (-CF₃) has a significant electronegativity value of 3.5, as measured by the Pauling scale.²⁷ The constituent F atoms are also known to enhance intermolecular C-F...H, F...S, C-F... π interactions.^{28, 29} Most importantly, -CF₃ can be easily introduced using 2,2,2-trifluoroethanol through esterification reaction. Therefore, it is rational to speculate the feasibility of introducing the -CF₃ group, as opposed to fluorine, in the molecular design of conjugated polymer donors. Despite great developments in the design of polymer donors, little work has been done to investigate the role of trifluoromethyl groups in polymer donors for solar cell applications.^{30, 31}

Herein, we designed and synthesized a trifluoromethylated polymer donor, poly[(2,6-(4,8-bis(5-(2-ethylhexyl)thiophen-2-yl)-benzo[1,2-*b*:4,5-*b'*])dithiophene))-*alt*-(2,5-(2,2,2-trifluoroethyl)thiophene carboxylate))] (**F1**), and its methylated variant, poly[(2,6-(4,8-bis(5-(2-ethylhexyl)thiophen-2-yl)-benzo[1,2-*b*:4,5-*b'*])dithiophene))-*alt*-(2,5-(ethyl thiophene carboxylate))] (**F0**). By comparing these two donors, we demonstrate that the -CF₃ group helps lower the HOMO energy level, increase absorption and improve intermolecular interactions. The two polymers were blended with a recently reported non-fullerene acceptor²², IT-4F (3,9-bis(2-methylene-((3-(1,1-dicyanomethylene)-6,7-difluoro)-indanone))-5,5,11,11-tetrakis(4-hexylphenyl)-dithieno[2,3-*d*:2',3'-

d']-s-indaceno[1,2-b:5,6-b']dithiophene), to fabricate PSCs. Optimized F1/IT-4F-based PSCs exhibit a maximum efficiency of 13.5 %, with a V_{oc} of 0.933 V, J_{sc} of 20.6 mA/cm² and FF of 70.0 %. In contrast, PSCs based on F0/IT-4F blends exhibit a maximum PCE of 4.9 %, with a V_{oc} of 0.832 V, J_{sc} of 13.5 mA/cm² and FF of 44.1 %.

Results and discussion

The synthesis routes of **F0** and **F1** are shown in **Figure 1**; synthetic details are included in the Supporting Information. The electron withdrawing monomer ester (**TMe** and **TFMe**) can be easily obtained via an esterification reaction using 2,5-dibromothiophene-3-carbonyl chloride and a corresponding alcohol with high yields (over 90%). Compared to fluorinating the aromatic rings on the conjugated core^{3,32}, introducing the trifluoromethyl (-CF₃) group to the conjugated core is easier. As shown in **Figure 1(d)** and **Figure S16**, reported aromatic fluorination of polymer donor is synthetically difficult. While in our case, non-aromatic fluorination from F0 to F1 needs fewer synthesis steps. Besides, this avoids high-cost and dangerous reagents, such as n-butyllithium (n-BuLi), lithium diisopropylamide (LDA) and N-fluorobenzenesulfonimide (NFSI). The polymers were prepared by Stille coupling-based polymerization of 2,5-dibromothiophene-3-ester and 4,8-Bis(5-(2-ethylhexyl)thiophen-2-yl)benzo[1,2-*b*:4,5-*b'*]dithiophene-2,6-diylbis(trimethylstannane) (BDTT). The polymers were then purified by Soxhlet extraction with methanol, hexanes, and finally extracted using chloroform. We determined the molecular weight of the polymers by high-temperature gel permeation chromatography (GPC) in *o*-dichlorobenzene at 145 °C with polystyrene as calibration standards. F0 and F1 exhibit number-average molecular weights (M_n) of 37.2 kg/mol (PDI = 2.1) and 40.3 kg/mol (PDI = 2.0), respectively. Both F0 and F1 are soluble in common solvents, including chloroform (CF), toluene (Tol) and chlorobenzene (CB).

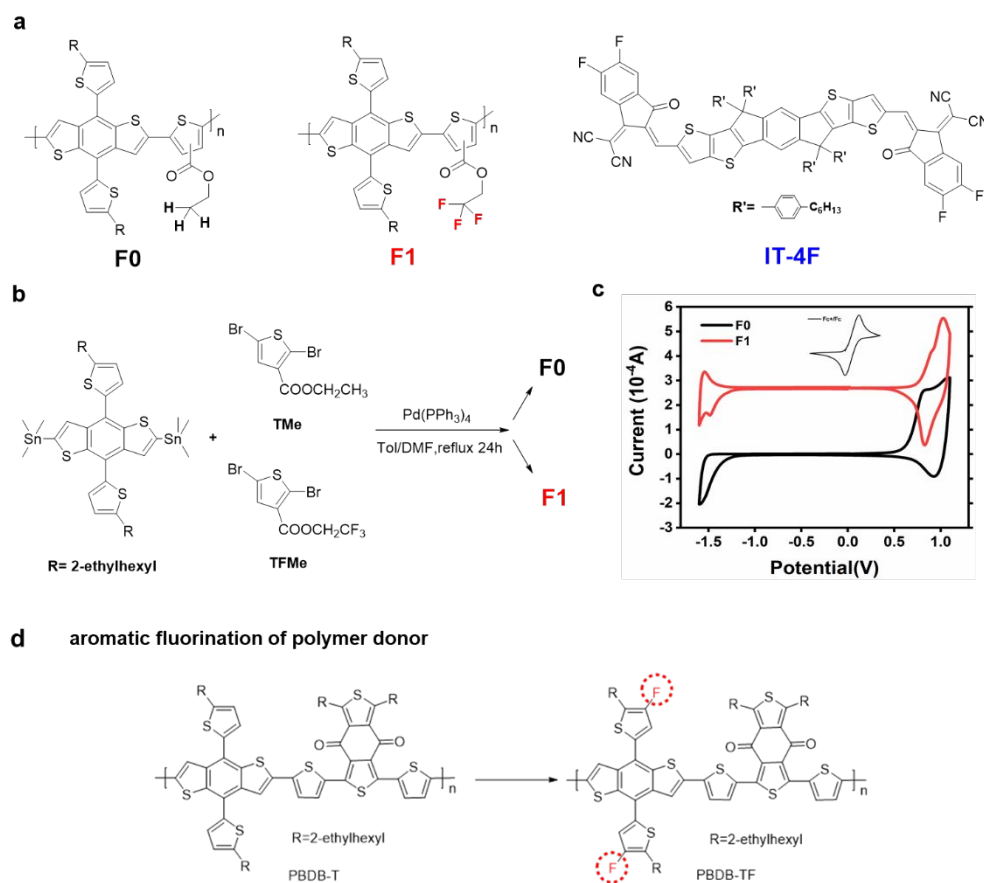


Figure 1. (a) Chemical structures of F0, F1, and IT-4F. (b) Chemical reaction yielding F0 and F1. (c) Cyclic voltammograms for F0, F1 and Fc⁺/Fc. (d) Aromatic fluorination of polymer donor.

To quantify the energy level differences between F0 and F1, we investigated their electrochemical properties through CV measurements. As shown in **Figure 1(c)**, the onset oxidation potential of F1 is 0.80 V, which is 0.15 V higher than that of F0. This observation indicates that introducing the electron-withdrawing -CF₃ group effectively lowers the HOMO energy level (E_{HOMO}) of the polymer donor from -5.35 eV (F0) to -5.50 eV (F1). The LUMO energy levels (E_{LUMO}) are calculated to be -3.35 and -3.53 eV for F0 and F1, respectively, extracted from E_{HOMO} and the optical bandgap. **Figure 2(a)** presents the solid-state absorption spectra of the two polymers as well as their solution spectra in chlorobenzene. In the solid state, F0 and F1 show similarly broad absorption from 450 nm to 600 nm with absorption edges ($\lambda_{\text{on-set}}$) at 620 nm and 630 nm, respectively, corresponding to an optical bandgap ($E_{\text{g}}^{\text{opt}}$) of 2.00 eV and 1.97 eV for F0 and F1. Both polymers exhibit strong π - π^* transition absorption maxima at around 520 nm (intrachain transition) and 580 nm (interchain transition)^{22, 33}. F1 is more absorptive; with an absorption coefficient of $1.25 \times 10^5 \text{ cm}^{-1}$ compared to that of F0 ($0.92 \times 10^5 \text{ cm}^{-1}$). Interestingly, the solution absorption profile of F1 is

similar to that of its solid state, whereas the solution absorption profile of F0 blueshifts substantially. This observation indicates that, in solution and at room temperature, F1 remains strongly aggregated. This aggregation persists, even when the solution is diluted to 0.001 mg/ml of F1 in CB, as shown in Figure S6.

To confirm that the introduction of $-CF_3$ enhances polymer aggregation, we measured the temperature-dependent absorption (TDA) spectra of F0 and F1 in CB. The absorption of F0 solution shows negligible temperature dependence. While for F1 solution, with increasing temperature from 30 to 80 °C, the absorption at 580 nm, which is assigned to interchain aggregation in F1, gradually disappears. Thermally reversible, this disaggregation results in a color change of the F1 solution from deep red to orange, as shown in the inset of **Figure 2(d)**. We attribute this TDA characteristic to the presence of dipole-induced Keesom interactions in F1. This interaction is temperature sensitive, the extent of which drastically decreases at high temperatures, likely as a result of increased twisting and disaggregation of F1.^{34 35} This Keesom interaction is reversible so F1 re-aggregates when the solution is cooled back to room temperature.

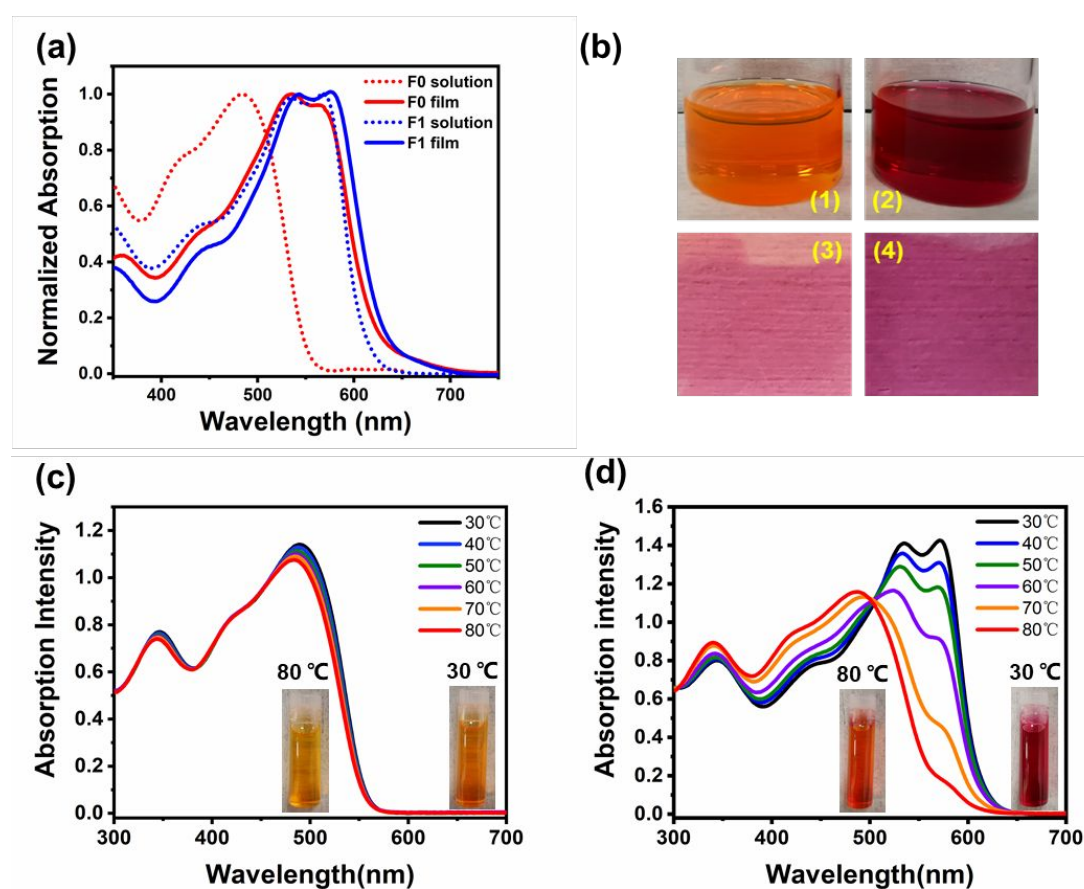


Figure 2. (a) UV-vis absorption spectrum of polymers. (b) (1)-(4) is picture of F0 solution, F1

solution, F0 thin film and F1 thin film. TDA spectra of (c) F0 and (d) F1.

Table 1. Optical parameters, frontier energy levels and molecular weights of the polymer donors.

Polymer	Sol ^a λ_{\max} (nm)	Film ^b λ_{\max} (nm)	Film ^b λ_{edge} (nm)	ϵ_{\max} ^b (10^5 cm^{-1})	$E_{\text{g}}^{\text{opt}}$ (eV)	HOMO ^c (eV)	LUMO ^d (eV)	M_n (kDa)	PDI
F0	484	535	620	0.92	2.00	-5.35	-3.35	37.2	2.10
F1	568	577	630	1.25	1.97	-5.50	-3.53	40.3	1.97

^a Chlorobenzene solution. ^b Thin films spin coated from chlorobenzene solution. ^c HOMO energy levels evaluated by CV using drop-casted thin films. ^d LUMO energy levels evaluated from HOMO and $E_{\text{g}}^{\text{opt}}$.

To evaluate the electrical properties of F0 and F1 as potential donors in polymer solar cells, we fabricated devices with an inverted structure of indium tin oxide (ITO)/ZnO/donor:acceptor/MoO₃/Ag. The processing conditions for the active layer, including the donor/acceptor (D/A) blend ratio, additive concentration and annealing temperature, were optimized individually (see Figure S3, S4 and S5 in Supporting Information). The device fabrication details can be found in Supporting Information. The current density-voltage (J - V) curves, external quantum efficiency (EQE) curves, and corresponding photovoltaic parameters of the optimized devices are shown in **Figure 3** and **Table 2**. As expected from the lower-lying HOMO level of polymer F1 compared to that of F0, the best performing BHJ solar cell with F1 exhibits a V_{oc} of 0.933 V that is higher than that of F0-based devices, whose record V_{oc} is 0.832 V. A J_{sc} of 20.6 mA cm⁻² can be achieved with the optimized F1-based device, while the J_{sc} is 13.5 mA cm⁻² for the best performing F0 solar cell. The increased J_{sc} of the F1-based device compared to the F0 device matches well with the broader and higher EQE response from 300 to 800 nm in F1-based devices, as presented in EQE curve (**Figure 3b**). For the F1-based devices, the EQE values in the range 520-760 nm exceed 75%, and the maximum EQE recorded at 590 nm is 83%. In contrast, the EQE values of F0-based PSCs lie consistently below 60%. The higher EQE values of F1/IT4F-based PSC possibly results from its stronger active layer absorption, as shown in Figure S3. Consequently, the best-performing F1-based device gives a PCE of 13.5% with a FF of 70.0%. Meanwhile, the best PSC based on F0/IT-4F only shows a PCE of 4.9% with a FF of 44.1%.

Balanced transport of electrons and holes plays a vital role in obtaining high FFs of PSCs³⁶. Hence, we investigated active-layer mobilities using the space charge-limited current (SCLC) method. Hole and electron-only devices were fabricated with structures of ITO/PEDOT:PSS/active layer/MoO₃/Ag and ITO/ZnO/active layer/PFN-Br/Al, respectively, to determine the hole mobility (μ_h) and electron mobility (μ_e) of the corresponding BHJ films (plotted in Figure S7, Supporting Information). The hole and electron mobilities of F1/IT-4F films are $(2.64 \pm 0.45) \times 10^{-4} \text{ cm}^2 \text{ V}^{-1} \text{ s}^{-1}$ and $(2.21 \pm 0.36) \times 10^{-4} \text{ cm}^2 \text{ V}^{-1} \text{ s}^{-1}$, respectively, which are both higher than those of F0/IT-4F films ($\mu_h = (3.72 \pm 0.33) \times 10^{-5} \text{ cm}^2 \text{ V}^{-1} \text{ s}^{-1}$, $\mu_e = (1.10 \pm 0.29) \times 10^{-4} \text{ cm}^2 \text{ V}^{-1} \text{ s}^{-1}$). F1-based devices exhibit more balanced charge-carrier mobilities, which is consistent with F1-based solar cells exhibiting higher FF.

Table 2. Photovoltaic parameters of optimized F0/IT-4F and F1/IT-4F devices under AM 1.5G illumination (100 mW cm^{-2}). The average values with standard deviations obtained from 15 devices are provided in the parentheses.

Blend	V_{oc} (V)	J_{sc} (mA/cm ²)	J_{cal} (mA/cm ²) ^a	FF (%)	PCE (%)
F0/IT-4F ^b	0.832	13.5	12.6	44.1	4.9
	(0.830 ± 0.004)	(13.4 ± 0.2)		(44.0 ± 0.4)	(4.6 ± 0.3)
F1/IT-4F ^{b,c}	0.933	20.6	19.9	70.0	13.5
	(0.929 ± 0.006)	(20.5 ± 0.2)		(69.5 ± 0.8)	(13.2 ± 0.3)

^a J_{cal} integrated from the EQE spectrum. ^b thermal annealed at 120 °C for 5 mins. ^c 0.5% DIO.

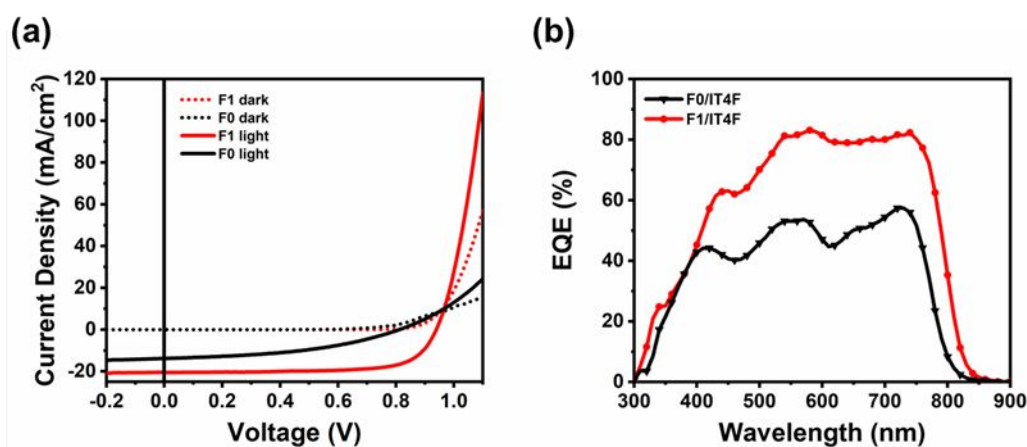


Figure 3. (a) J - V curves and (b) EQE curves of F0/F1-based PSCs.

We investigated the morphological characteristics of the neat films and blends of F1 and F0 with

IT-4F through grazing-incidence wide-angle scattering (GIWAXS), the results of which are summarized in **Figure 4**. All of these films exhibit limited long-range ordering. We made the following assignments, based on the typical packing structure of this class of low-crystalline donor-acceptor polymers.³⁷⁻⁴⁰ The GIWAXS pattern of neat F0 film, as shown in **Figure 4(a)**, shows a broad reflection at $q = 0.37 \text{ \AA}^{-1}$ in the out-of-plane direction, attributable to weak side-chain stacking of F0. In contrast, as shown in **Figure 4(b)**, the diffraction of F1 film exhibits increased ordering than F0 film; in addition to the reflection at $q = 0.29 \text{ \AA}^{-1}$ in the in-plane direction due to side-chain stacking order in F1, we also observe a reflection at $q = 1.62 \text{ \AA}^{-1}$ (d -spacing: 3.88 \AA) in the out-of-plane direction, which corresponds to pi-pi stacking characteristic in F1 with a preference to be normal to the substrate. As shown in **Figures 4c-d**, the respective blends of F0 and F1 with IT-4F exhibit similar trends; F1/IT4F blend film shows enhanced ordering than F0/IT4F blend film.

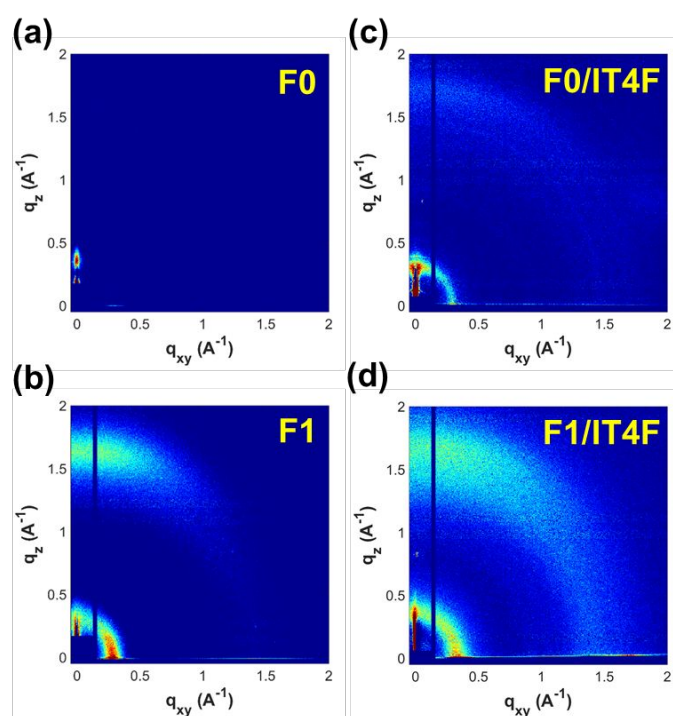


Figure 4. GIWAXS pattern of (a) F0 film, (b) F1 film, (c) F0/IT-4F blends and (d) F1/IT-4F blends.

To gain an understanding of the structural differences induced by the introduction of a trifluoromethyl group ($-\text{CF}_3$) in the polymers at the molecular level, we performed density functional theory (DFT) calculations of their oligomeric models, the results of which are shown in **Figure 5**. Both polymers exhibit a largely planar backbone conformation with a dihedral angle

between two adjacent thiophene units of around 5° . That these polymers are conformationally similar is not surprising given that the steric hindrance of $-\text{CF}_3$ is not significantly larger than that of $-\text{CH}_3$. We calculated molecular energy levels of F0 and F1 based on one to three polymer repeating units, respectively (see in Figure S15). Yet, given its strong electron-withdrawing properties, the introduction of $-\text{CF}_3$ leads to lower HOMO/LUMO levels in F1 compared to those in F0, consistent with the CV measurements discussed above.

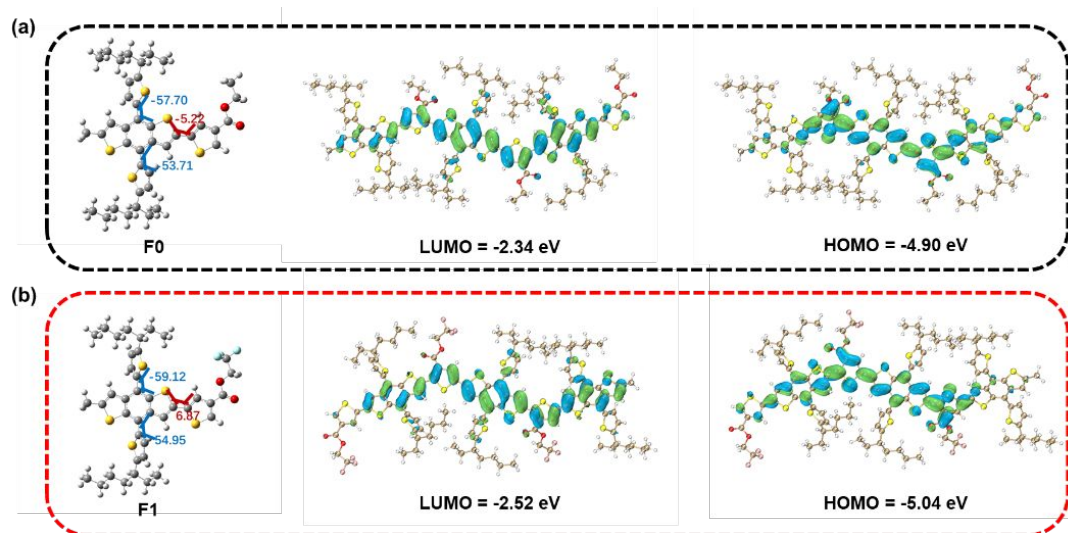


Figure 5. Molecular configurations and calculated frontier molecular orbitals of polymers based on three repeat units carried out by DFT at the B3LYP/6-31g (d, p) level.

Conclusion

In summary, we introduced $-\text{CF}_3$ as a facile and simple fluorination way of altering the intermolecular packing and optoelectronic properties of a polymer donor. This strategy does not require complicated multi-step synthetic procedures, but it produces a polymer donor that has a lower HOMO energy level, increased absorption, and stronger intermolecular interactions. Concurrent to the changes in these properties is a substantial improvement in device performance when this polymer donor is incorporated in solar cells compared to its methylated counterpart. These findings may contribute to developing new high-performance polymer donor materials through introducing trifluoromethyl group into other acceptor units.

Acknowledgements

H. M. acknowledges the Shenzhen Hong Kong Innovation Circle joint R & D project

(SGLH20161212101631809), China (Shenzhen)-Canada Technology Collaboration Project (GJHZ20180420180725249), The China (Shenzhen)-United States Technology Collaboration Project (GJHZ20180928163206500).

C. Y. thanks the support from China Scholarship Council (CSC File No. 201806010248).

K.G. and Y.-L.L. acknowledge partial funding from the Princeton Center for Complex Materials, a MRSEC supported by the NSF under Award DMR-1420541. K.G. acknowledges the Mr. and Mrs. Yan Huo *94*95 Graduate Fellowship, administered by Princeton Institute for International and Regional Studies (PIIRS). We appreciate Dr. E. Tsai's help on the X-ray scattering measurements. The research used the Center for Functional Nanomaterials (CFN) and the Complex Materials Scattering (CMS) beamline of the National Synchrotron Light Source II (NSLS-II), which both are U.S. DOE Office of Science Facilities, at Brookhaven National Laboratory under Contract No. DE-SC0012704.

D.-F. P acknowledges the support from the Peng Cheng Scholarship.

Conflict of Interest

The authors declare no conflict of interest.

Key words

polymer donor, organic solar cells, trifluoromethyl group, dipole-dipole interactions

1. L. Lu, T. Zheng, Q. Wu, A. M. Schneider, D. Zhao and L. Yu, *Chemical Reviews*, 2015, **115**, 12666-12731.
2. S. Xiao, Q. Zhang and W. You, *Advanced Materials*, 2017, **29**, 1601391.
3. H. Yao, L. Ye, H. Zhang, S. Li, S. Zhang and J. Hou, *Chemical Reviews*, 2016, **116**, 7397-7457.
4. Y. Lin, Q. He, F. Zhao, L. Huo, J. Mai, X. Lu, C.-J. Su, T. Li, J. Wang, J. Zhu, Y. Sun,

- C. Wang and X. Zhan, *Journal of the American Chemical Society*, 2016, **138**, 2973-2976.
5. M. Li, Y. Liu, W. Ni, F. Liu, H. Feng, Y. Zhang, T. Liu, H. Zhang, X. Wan, B. Kan, Q. Zhang, T. P. Russell and Y. Chen, *Journal of Materials Chemistry A*, 2016, **4**, 10409-10413.
6. Y. Li, X. Liu, F.-P. Wu, Y. Zhou, Z.-Q. Jiang, B. Song, Y. Xia, Z.-G. Zhang, F. Gao, O. Inganäs, Y. Li and L.-S. Liao, *Journal of Materials Chemistry A*, 2016, **4**, 5890-5897.
7. J. Wang, W. Wang, X. Wang, Y. Wu, Q. Zhang, C. Yan, W. Ma, W. You and X. Zhan, *Advanced Materials*, 2017, **29**, 1702125.
8. Y. Lin, T. Li, F. Zhao, L. Han, Z. Wang, Y. Wu, Q. He, J. Wang, L. Huo, Y. Sun, C. Wang, W. Ma and X. Zhan, *Advanced Energy Materials*, 2016, **6**, 1600854.
9. N. Qiu, H. Zhang, X. Wan, C. Li, X. Ke, H. Feng, B. Kan, H. Zhang, Q. Zhang, Y. Lu and Y. Chen, *Advanced Materials*, 2016, **29**, 1604964.
10. C. Yao, B. Liu, Y. Zhu, L. Hong, J. Miao, J. Hou, F. He and H. Meng, *Journal of Materials Chemistry A*, 2019, **7**, 10212-10216.
11. J. Yuan, Y. Zhang, L. Zhou, G. Zhang, H.-L. Yip, T.-K. Lau, X. Lu, C. Zhu, H. Peng, P. A. Johnson, M. Leclerc, Y. Cao, J. Ulanski, Y. Li and Y. Zou, *Joule*, 2019, **3**, 1140-1151.
12. Y. Cui, H. Yao, J. Zhang, T. Zhang, Y. Wang, L. Hong, K. Xian, B. Xu, S. Zhang, J. Peng, Z. Wei, F. Gao and J. Hou, *Nature Communications*, 2019, **10**, 2515.
13. T. L. Nguyen, H. Choi, S. J. Ko, M. A. Uddin, B. Walker, S. Yum, J. E. Jeong, M. H. Yun, T. J. Shin, S. Hwang, J. Y. Kim and H. Y. Woo, *Energy & Environmental Science*,

- 2014, **7**, 3040-3051.
14. J. W. Jo, J. W. Jung, E. H. Jung, H. Ahn, T. J. Shin and W. H. Jo, *Energy & Environmental Science*, 2015, **8**, 2427-2434.
 15. Y. Zhang, S.-C. Chien, K.-S. Chen, H.-L. Yip, Y. Sun, J. A. Davies, F.-C. Chen and A. K. Y. Jen, *Chemical Communications*, 2011, **47**, 11026-11028.
 16. A. C. Stuart, J. R. Tumbleston, H. Zhou, W. Li, S. Liu, H. Ade and W. You, *Journal of the American Chemical Society*, 2013, **135**, 1806-1815.
 17. J. R. Tumbleston, B. A. Collins, L. Yang, A. C. Stuart, E. Gann, W. Ma, W. You and H. Ade, *Nature Photonics*, 2014, **8**, 385.
 18. H.-Y. Chen, J. Hou, S. Zhang, Y. Liang, G. Yang, Y. Yang, L. Yu, Y. Wu and G. Li, *Nature Photonics*, 2009, **3**, 649.
 19. J. Liu, S. Chen, D. Qian, B. Gautam, G. Yang, J. Zhao, J. Bergqvist, F. Zhang, W. Ma, H. Ade, O. Inganäs, K. Gundogdu, F. Gao and H. Yan, *Nature Energy*, 2016, **1**, 16089.
 20. H. Fu, Z. Wang and Y. Sun, *Angewandte Chemie International Edition*, 2019, **58**, 4442-4453.
 21. X. Xu, K. Feng, Z. Bi, W. Ma, G. Zhang and Q. Peng, *Advanced Materials*, 2019, **31**, 1901872.
 22. W. Zhao, S. Li, H. Yao, S. Zhang, Y. Zhang, B. Yang and J. Hou, *Journal of the American Chemical Society*, 2017, **139**, 7148-7151.
 23. M. Zhang, X. Guo, W. Ma, H. Ade and J. Hou, *Advanced Materials*, 2015, **27**, 4655-4660.
 24. Y. Liang, D. Feng, Y. Wu, S.-T. Tsai, G. Li, C. Ray and L. Yu, *Journal of the American*

- Chemical Society*, 2009, **131**, 7792-7799.
25. M. L. Tang and Z. Bao, *Chemistry of Materials*, 2011, **23**, 446-455.
26. D. Mo, H. Wang, H. Chen, S. Qu, P. Chao, Z. Yang, L. Tian, Y.-A. Su, Y. Gao, B. Yang, W. Chen and F. He, *Chemistry of Materials*, 2017, **29**, 2819-2830.
27. M. A. McClinton and D. A. McClinton, *Tetrahedron*, 1992, **48**, 6555-6666.
28. K. Reichenbacher, H. I. Süss and J. Hulliger, *Chemical Society Reviews*, 2005, **34**, 22-30.
29. Y. Wang, S. R. Parkin, J. Gierschner and M. D. Watson, *Organic Letters*, 2008, **10**, 3307-3310.
30. W. Li, G. Li, X. Guo, Y. Wang, H. Guo, Q. Xu, M. Zhang and Y. Li, *Journal of Materials Chemistry A*, 2018, **6**, 6551-6558.
31. P. Deng, Z. Wu, K. Cao, Q. Zhang, B. Sun and S. R. Marder, *Polymer Chemistry*, 2013, **4**, 5275-5282.
32. H. Zhou, L. Yang, A. C. Stuart, S. C. Price, S. Liu and W. You, *Angewandte Chemie International Edition*, 2011, **50**, 2995-2998.
33. D. Qian, L. Ye, M. Zhang, Y. Liang, L. Li, Y. Huang, X. Guo, S. Zhang, Z. a. Tan and J. Hou, *Macromolecules*, 2012, **45**, 9611-9617.
34. F. L. Leite, C. C. Bueno, A. L. Da Róz, E. C. Ziemath and O. N. Oliveira, *International Journal of Molecular Sciences*, 2012, **13**.
35. H. Hu, P. C. Y. Chow, G. Zhang, T. Ma, J. Liu, G. Yang and H. Yan, *Accounts of Chemical Research*, 2017, **50**, 2519-2528.
36. M. Abbas and N. Tekin, *Applied Physics Letters*, 2012, **101**, 073302.

37. X. Guo, N. Zhou, S. J. Lou, J. Smith, D. B. Tice, J. W. Hennek, R. P. Ortiz, J. T. L. Navarrete, S. Li, J. Strzalka, L. X. Chen, R. P. H. Chang, A. Facchetti and T. J. Marks, *Nature Photonics*, 2013, **7**, 825.
38. H. Bin, Z.-G. Zhang, L. Gao, S. Chen, L. Zhong, L. Xue, C. Yang and Y. Li, *Journal of the American Chemical Society*, 2016, **138**, 4657-4664.
39. L. Lu and L. Yu, *Advanced Materials*, 2014, **26**, 4413-4430.
40. C. Sun, F. Pan, H. Bin, J. Zhang, L. Xue, B. Qiu, Z. Wei, Z.-G. Zhang and Y. Li, *Nature Communications*, 2018, **9**, 743.